28th AIAA Applied Aerodynamics Conference
28 June - 1 July 2010, Chicago, Illinois

AIAA 2010-4686

Development and Testing of Deployable Vortex Generators Using SMA Actuation

Todd R. Quackenbush[1], Robert M. McKillip, Jr.[2], and Glen R. Whitehouse[3]
Continuum Dynamics, Inc.
Ewing, NJ 08618
todd@continuum-dynamics.com

Fixed-vane vortex generators (VGs) have been in existence for over 50 years and are still among the most effective available flow control devices. However once such fixed VGs have been configured to improve performance in one regime, they often penalize the performance in other conditions. This paper will summarize results of an effort making VGs deployable "on demand". The technology enabling this improvement is the use of Shape Memory Alloy (SMA) based actuators to deploy Pop Up Vortex Generators (PUVG). Because of the favorable force/stroke characteristics of SMA actuators, it is possible to design PUVGs so that they retract flush to the wing surface and so have negligible aerodynamic penalty when not deployed. In addition, novel self-locking actuation devices enable deployment of PUVGs to be maintained with no power expenditure. This paper summarizes the design, construction, and demonstration of practical PUVG devices. Wind tunnel tests of a near full scale wing with an array of PUVGs are described, illustrating a substantial mitigation of flow separation and demonstrating enhanced lift as well as improved lift/drag ratio at flow conditions representative of general aviation aircraft.

Nomenclature

c	wing chord, ft.
$c_{\ell_{max}}$	maximum lift coefficient
h	vortex generator device height, ft.
Re_x	boundary layer Reynolds number, Vx/ν
V	free stream speed, ft./sec.
x	distance along boundary surface, ft.
/ν	wing angle of attack, rad.
/ν$_{c\ell_{max}}$	angle of attack for maximum lift, rad.
/ν$_{0\ell}$	angle of attack for zero lift, rad./ν
/ν	boundary layer thickness, ft.
/ν	kinematic viscosity, ft./sec.

I. Introduction

Improved high lift and cruise performance of commercial, military, and general aviation aircraft offers a tremendous potential payoff in terms of reducing operating costs. One of the central technical issues in both for enhanced cruise as well as high lift and maneuvering performance is the reduction or elimination of boundary layer separation. Regarding cruise drag for fixed wing aircraft, it has been estimated that each 1% reduction of cruise drag will yield a savings of roughly 1.3 million gallons of fuel over the life of an aircraft.[1] Since 1% of aircraft drag coefficient is 2-3 drag counts for a typical transport in cruise, it is clear that even modest improvements can have a very substantial payback in reduced operating costs. Thus, minimization of drag for cruise flight has been a central preoccupation of aircraft designers for many years, and concerns have heightened given the recent environment of unstable fuel prices, which puts extreme pressure on operational costs for both civilian and military operators. The drag budgets of particular aircraft vary significantly, but the primary components of drag for subsonic transports are skin friction drag and drag due to lift, which compose roughly 50 and 35 percent of total drag in cruise, respectively.[2] Significant strides have been made in reducing these quantities through fuselage streamlining, airfoil selection, as well as in the optimization of engine nacelle installation and wing root filleting. However, as is made clear in several reviews,[3-5] the large volume of past and ongoing research in drag reduction[6-11] indicates substantial room for improvement.

[1,2] Senior Associate, Continuum Dynamics, Inc. Senior Member, AIAA.
[3] Associate, Continuum Dynamics, Inc. Member, AIAA.

Enhanced lift is also a critical issue, both for commercial jetliners and general aviation aircraft. Efforts have been underway for many years to simplify the complex, multi-component flaps typically used to obtain the high lift coefficients and low landing speeds desired for civil transports. Devices that can maintain attached flow over key flap components could in principle offer the possibility of eliminating one or more components of the current generation of double- or triple-slotted flaps. The payoff in reduced weight and complexity from such a design breakthrough would be substantial.

Lift enhancement on landing would have a particularly high payoff for General Aviation (GA) aircraft, since the reduced landing speed that would result would both simplify the task of GA pilots, easing the overall piloting task, and simultaneously make shorter airfields accessible, broadening the range of possible airstrips for wider use of GA aircraft. Flow control technology for GA applications, however, must necessarily be low cost and simple to implement, given the limits on cost and system complexity that inevitably go with light aircraft.

Both drag mitigation and lift enhancement at root require control of flow separation. Fixed-vane vortex generators (VGs) have been used for almost half a century and are still among the most effective available flow control devices. However, they suffer from the inherent limitation that once such fixed VGs have been optimized for one flight regime, they often penalize the performance in other operational flight conditions. The effort described here sought to improve upon the fixed VG by making it deployable "on demand" and thereby eliminating any penalty when the generators are not needed. As has been discussed in prior research[12], the potential benefits of developing active or deployable VGs are substantial; however, they are best implemented by device technology requiring minimal power and simple control systems. Moreover, they must be weighed against the capabilities of alternative approaches to flow control, which are now briefly reviewed.

II. Technical Background

A considerable fraction of the most common passive design approaches to separation controla (e.g., streamlining, use of laminar flow airfoils, filleting, optimization of nacelle/wing interference, etc.) have been exploited to date. Thus, attention is turning to active measures and here a variety of approaches have been studied. For example, it is well known that there are a wide range of devices which introduce steady vortex structures or use steady blowing to energize boundary layers so as to postpone or even prevent flow separation. Included in this class of devices are slotted flaps, slats, and turbulators, which have enabled engineers to reduce the minimum airspeed at which an airplane can maneuver. With these devices a jet of fluid between wing segments provides an excess of momentum in the wall region which can promote flow attachment.

Steady active tangential blowing with slots or jets has also been demonstrated - in a range of laboratory flight settings - to delay separation and enhance lift. In recent years, great strides have been made in the development of active control blowing concepts for control of boundary layer separation and free shear layer mixing processes. Low Mach number and Reynolds number experiments have demonstrated that cyclic vortical oscillations introduced into a separating boundary layer slightly upstream of the average separation location can effectively delay boundary layer separation. Seifert et al.,[13] and later, Seifert and Pack[14] have demonstrated that for single and two-element airfoils, cyclic slot blowing greatly enhanced the delay of boundary layer separation. Similar delay in boundary layer separation has been demonstrated by McManus et al[15] using pulsed vortex generator jets.

Unfortunately, both steady and oscillatory blowing concepts typically require actuation devices which, while successful in a laboratory setting, have been difficult to implement in flight applications of interest. For example, direct blowing has very limited practical application due to the large momentum ratios required, cost and weight penalties associated with delivering large volumes of air to the required location, and the power requirements necessary to provide such air supplies.[16] A variation on pulsed vortex generator jets are synthetic jets which are actuated by small diaphragm driven cavities below the jet orifice. The cyclic flow structures introduced by synthetic jets are similar to pulsed jets with the predominant introduction of longitudinal vorticity.[17] While these devices have been demonstrated for low speed and low Reynolds number applications, generating the mechanical forces (momentum coefficients) necessary for real aircraft transonic flow regimes has proved difficulty. Given these limitations, it has been judged important to revisit the design of older VG concepts and to ensure that all possible variations have been exploited.

Classical fixed VGs introduce streamwise vorticity within or at the edge of the boundary layer, which in turn, transfers high momentum fluid from the outer flow to the wall region to delay boundary layer separation.

Taylor first introduced VGs consisting of a row of small plates or airfoils oriented normal to the surface and set at an angle of incidence to the local flow.[18] Typically the height, h, of these devices is on the order of the boundary layer thickness, /ν. Work by Lin[9,19] has shown that VGs can be designed with much smaller heights (called micro-VGs with h//ν as low as 0.2) while maintaining their effectiveness and yielding a significant reduction in associated drag for high-lift configurations when applied directly to flap segments. Lin studied a wide range of passive flow control devices, judging their relative effectiveness in separation control for a backward facing step. This work concluded that the most effective group of flow separation control devices were those that generate streamwise vortices, such as those produced by the conventional and micro-VGs. VGs have been used to delay boundary layer separation, to enhance aircraft wing lift, to improve aircraft stability, to reduce drag on fuselages and ship hulls, and on nacelles and inlets to improve engine performance.[20] To date many of these applications use relatively large VGs (order h//ν~1) which results in significant drag penalties for aircraft and pressure losses for inlets under cruise conditions when the VGs are not required. It is important to note at this point that, due to their small size, /νGs are particularly well suited to active deployment/retraction and flush surface stowage with minimal body intrusion or flow disturbance.

To summarize, many of the active concepts discussed above and in the cited references have practical drawbacks in terms of their mechanical implementation on aircraft and the installation penalties associated with required power, hardware weight, and hardware complexity. VGs, on the other hand, are a proven technology for the management of flow separation, drag reduction, and improved maneuvering performance in a wide range of aerospace and marine applications. As noted above, fixed or passive VG devices typically provide beneficial flow effects only in a narrow set of flight conditions (e.g., delay of separation under high lift conditions, improved handling, reduction of body separation, improved engine performance). This places a high priority on "deployment on demand" where VG//νGs are selectively deployed as needed and otherwise stowed flush with the surface.

Figure 1 shows a simple application of a generic Pop Up Vortex Generator (PUVG) to separation control over a wing (one can imagine similar installations on fuselages, nacelles, and other separation prone regions). With the pop-up concept, the VGs are constructed to fold up or down on the surface of the wing only when and where needed, as suggested schematically in Figure 1. The ability to retract or fold the VGs (installed to increase lift during landing) would remove a significant cruise performance penalty. To be commercially successful for both new and existing aircraft it is critical for prospective PUVG devices to meet the following requirements: (1) the device must stow flush with the mold-line of the mounting surface; (2) the device should have minimal intrusion below the surface on which it is mounted (ideally no below surface intrusion); and (3) the device must not require complex and bulky power leads (no hydraulic lines or mechanical activation devices); and (4) simple control and zero power requirement for holding position are ideal for practical implementation. Recent developments in the use of smart materials technology, coupled with novel self-locking mechanisms, have made such a development possible, as will now be described.

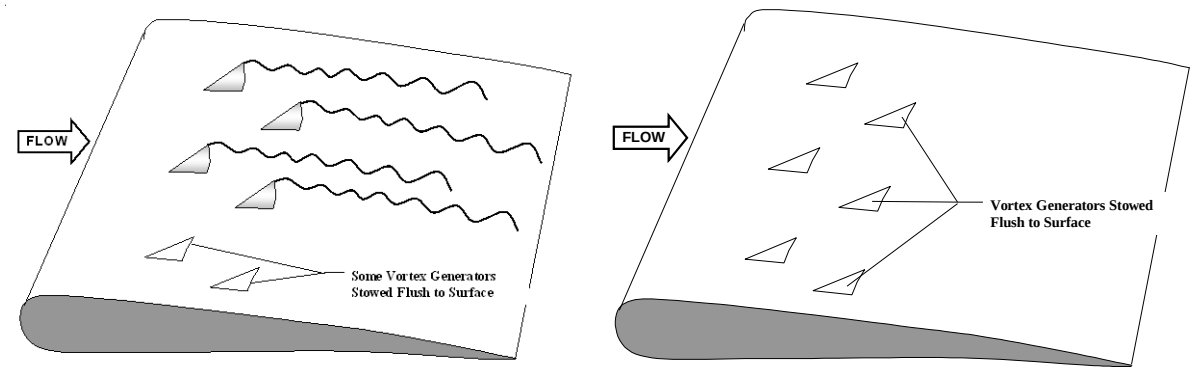

Figure 1. Array of Pop-Up Vortex Generators (PUVG) deployed (left) and stowed (right). Note that VGs can be individually deployed and stowed.

III. Overview of SMA Materials

A critical consideration for candidate PUVGs is selection of the most appropriate actuator designs. Effective and robust actuation for this application can be achieved with an absolute minimum of mechanical complexity through the use of SMA technology, a subset of what is commonly known as "smart structures". "Smart" materials have been the subject of several recent investigations for use as actuators in aerodynamic, aeroelastic, and acoustic applications.[23-32]. Piezoceramic materials feature very high frequency response but suffer from limited control power due to small crystal displacements. SMAs, by contrast, have the attractive feature of providing significant (on the order of 2-5%) strain capability, which makes them useful as "smart" actuators for aerodynamic surfaces and vortex generators. Research into their use as actuation devices for a variety of applications has shown them to be practical alternatives to the more limited motion piezoelectric devices.[33] SMA actuators not only provide relatively high strains, but also can provide large forces in lightweight, low volume packages that require low voltages and modest power to operate.

The most practical shape memory materials are alloys of nickel and titanium, which exist in one of two stable crystalline phases: a high temperature 'austenite' and a low temperature 'martensite'. The two phases have dramatically different stress-strain curves (Figure 2). The austenitic phase has a conventional stress-strain curve with a higher modulus of elasticity while the martensitic phase exhibits a stress plateau between two yield points. If the SMA is mechanically deformed in its martensitic phase, it will return to its original shape when its temperature is raised. If the SMA is constrained from returning to its original shape then a stress is generated on heating through its transformation temperature. Phase transformation temperatures of 70-90˚C are common with the martensite phase typically occurring at room temperature (Figure 3).

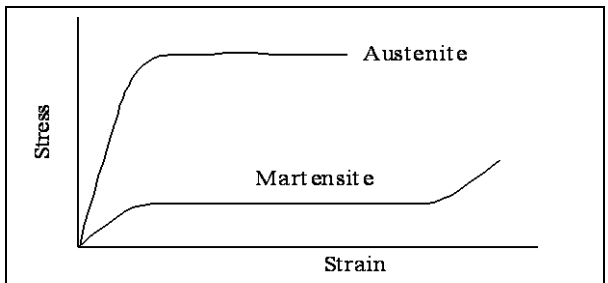

Figure 2. Schematic of a typical stress/strain curve for NiTi SMA in its two material phases.

The net effect of these properties is that SMA wires can adjust their length as a function of temperature under load, producing high control forces in the process. Heating of SMA wires is typically accomplished by passing a current through them, with cooling done either by natural convection or embedding the wires in high heat sink material. Literature on applications of shape memory materials to date includes a variety of static load deflection applications as well as control of structural vibrations at up to 10 Hz.[26]. In addition, SMA devices have demonstrated the ability to produce large control forces and substantial deflections while retaining long cycle life.

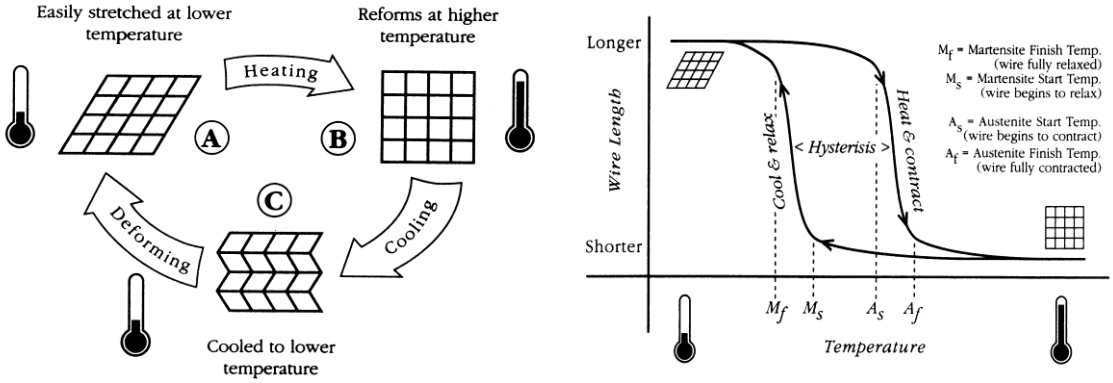

Figure 3: Schematic of SMA phase change (left) and material properties (right).

IV. Device Development Supporting PUVGs

A wide range of prior projects by the present authors have established a substantial engineering knowledge base for SMA actuator design and construction[27-32]; this includes (1) extensive materials testing (e.g., wire stress/strain analysis, repeatability, sensitivity to thermal environment); (2) generation of aero-thermal-elastic models for airfoil deflection with embedded actuators; (3) integration studies for candidate actuator designs; and (4) bench top testing of demonstration devices. In particular, a recent project implementing rotor vibration reduction using SMA-driven devices for individual blade control on helicopters[27] produced technology critical to PUVG development. Here, the focus was on a scheme to actively control rotor one-per-rev vibration and blade tracking through use of variable geometry trailing tabs.

The key innovation from this effort included a zero-power "snap-through" actuation design for these tabs, and this concept is described referred to in Figure 4. Shown in Figure 4a is a flat plate element which is notched such that when points A-B are forced together the surface buckles elastically into one of two positions (the downward deflection is shown in Figure 4b). The deflection results from the prestress which is introduced in the plate, and studies to date have shown that deflection angles of $\pm 25/\nu$ are achievable for acceptable levels of plate stress. Figure 4c schematically shows the addition of pre-strained SMA actuator wires attached to the upper and lower surfaces. Assuming the plate is initially buckled downward as shown in Figure 4b, heating the top SMA wire will cause it to shorten and the plate will "pop-through" and lock in the upward buckled position. The innovations in this actuator are two-fold:

/v The structural or load-bearing component of the actuator is a very simple machine (a notched flat plate). This component is readily fabricated and encapsulated to form a useful aerodynamic surface.

/v Power is only required to transition the actuator from one position to its second position. Once the transition is made the power to the actuating wire is cut-off and the actuator is locked into position by the stressed plate.

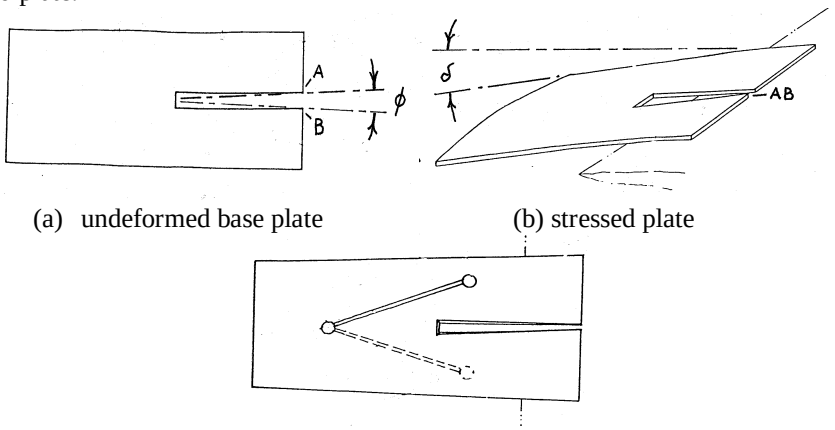

(a) undeformed base plate (b) stressed plate

(c) tab with SMA wires installed

Figure 4. Schematic of "snap-through" trailing edge tab[28] .

The device described above is ideal for continuous deployment, since once self-locked, zero power is required. An early-stage demonstrations is shown in Figure 5, where three bi-modal tabs are installed along the trailing edge of a helicopter blade. The tabs are snapped into one of two positions until it is observed that each blade tip travels in the same tip path plane, thereby reducing one/rev vibration. The trim function is actively controlled without stopping the rotor rotation. As is described in several recent publications [27,28,32] multiple additional applications of this device are possible. A practical demonstration of the effectiveness of this device came during ground tests on full scale autogyro blades (Figure 6). A set of snap-through tabs were mounted on the trailing edge of the blades of a 20 ft. diameter rotor system on a Benson light autogiro, and the rotor system was operated at 200 RPM, producing flow speeds of over 150 fps and lateral G loadings in excess of 100. The snap-through tabs produced repeatable deflection performance even under these challenging operating conditions.

The success of this device suggested a possible development path for a self-locking PUVG design that could bypass the limitation of prior deployable VGs[9,32] that required continuous power during operation. Before detailing this configuration, however, it is important to establish the likely dimensions of the surface. Review of existing literature on vortex generator design and applications[35-39] indicated that a basic parameter for scaling the height h of vortex generators on wings was to select h/c of approximately .01, where c is the wing chord. From the point of view of potential wind tunnel testing, a balance of maximum size constraints and generation of realistic Reynolds numbers (considerations discussed in the following sections) indicated roughly a 2 ft. (24") chord would be a reasonable estimate for a wing test article. Thus, estimated PUVG height (when deployed) would be roughly 250 mils (0.25") for this application, though clearly different size devices would be called for given different installation situations. By extension, the desired deflection serves to scale the approximate length scale L for the VGs themselves, indicating that the length of the VG from the attachment point to the trailing edge should be approximately 0.8-1.0 inches; overall length would be roughly 1.5" (allowing for the VG structure forward of the attachment); the appropriate width scales up to be roughly 1".

Figure 5. SMA-driven bi-modal tabs mounted to trailing edge of a CH-47 blade section.

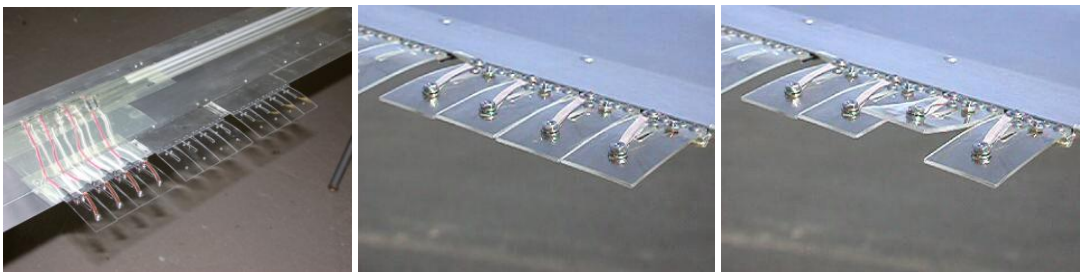

Figure 6. A series of snap-through actuators used as trim tabs in the autogiro ground test.

An initial large scale (~6" long) mechanical device that illustrates the principles of potential PUVG is shown in Figure 7, along with the first steps toward scaling down this concept; here, (non-powered) self-locking PUVGs are shown in two variations - two flush-mounted and two surface-mounted, with the retracted and deployed states of each configuration shown. Sizing and construction of these (manually operated) devices were the first steps in fabrication of devices suitable for testing on wings in the flow domains of most interest for this application (e.g., GA aircraft at typical landing speeds). The major dimensions of these particular demonstration devices were roughly 1-1.5 inches.

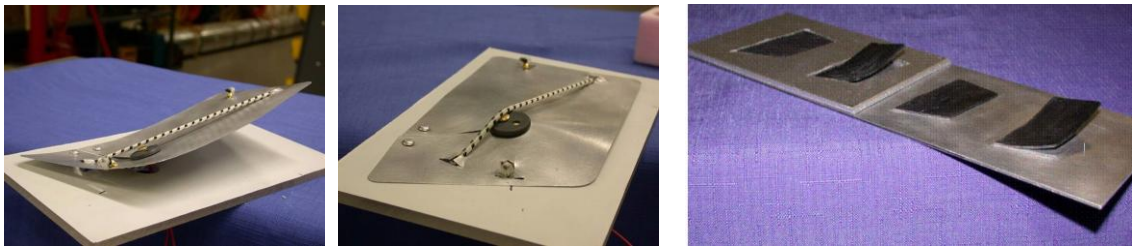

Figure 7. Large-scale (left) and small-scale (right) mechanical demonstrator for snap-through PUVG prototypes.

Another key consideration was ensuring that the actual design lies below the height of the actual boundary layer when retracted. Assuming for design purposes that the VGs are mounted at the 25% chord location of a 24" chord wing, a first estimate for fully developed turbulent boundary layer thickness is /νx/ν

$= 0.4\ (Re_x)^{-0.2}$. Re_x for a 100 fps onset speed is 375,000, leading to an estimated boundary layer thickess of 0.15 in. at this point. Scaling the likely retracted height from Figure 7 to be roughly 0.2h or 0.06L, this makes the estimated retracted PUVG height roughly 0.06", well below the estimated boundary layer height.

V. PUVG Fabrication and Initial Testing

Based on the scaling studies just described, drawings were developed for candidate actuators (e.g., Figure 8). One important aspect of developing this design was the thickness required to balance the requirements of stiffness (to hold shape under aerodynamic load) and flexibility (to respond for realizable actuator force levels). Limited modeling and in-shop testing with various gauges of steel indicated that thicknesses in the .003-.007" range were potential candidates, depending on actuators available and the flow speeds. For the dynamic pressures of interest for this application, the .005" thickness - at the middle of this range - appeared to be the best solution. The next logical step was testing of initial installation and actuation with SMA wire. Figure 8 shows the schematic of powered installation with a top view showing the upper surface wire that provides pop-up actuation; pop-down is provided by a wire symmetrically located on the lower surface. Figure 9 shows the deployed and retracted geometries for the PUVG installed on a 1/16th" thick aluminum plate. The actuation wire used is .01" dia. ball-end nickel titanium SMA wire specifically tailored for this application. Application of current produced repeatable deflection for this demonstrator, with roughly 3 amps of input current required.

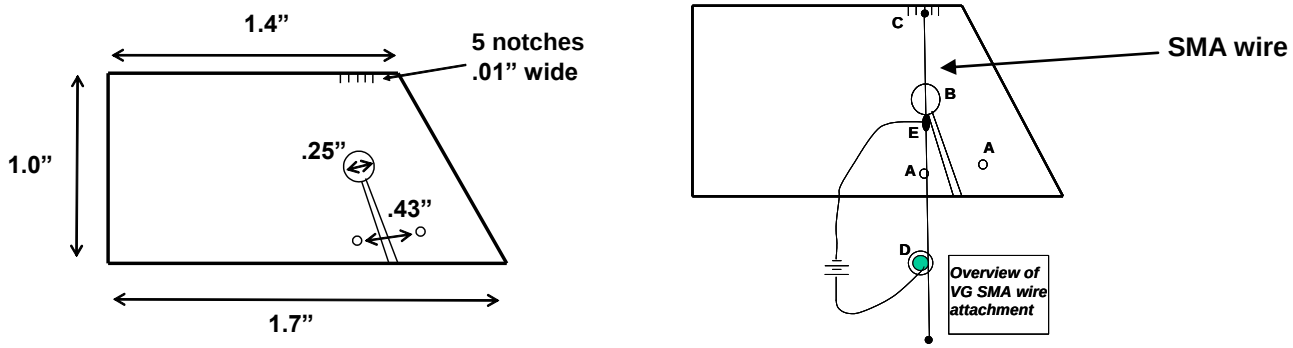

Figure 8. (left) Dimensions of initial benchtop PUVG demonstrator; (right) plan view of SMA actuated PUVG installation. (note: symmetrical wire installation providing retraction not shown)

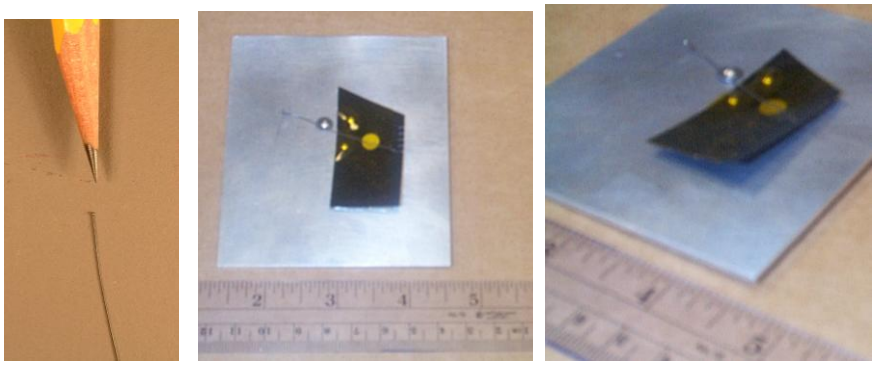

Figure 9. Overall views of test article used in powered demonstrations.

Prior experience has indicated that a substantial onset flow produces sufficient convective cooling to significantly increase the current required to achieve transition. The next step in our testing process, then, was to expose these PUVGs to appropriate levels of flow in a low speed 1'x1' wind tunnel (Figure 10). These tests indicated that onset flows above roughly 50 fps would increase the required current to as much a 5A, though the exact level was somewhat dependent on the extent of cabling supplying the PUVG array. Cooling losses could be reduced, however, with the use of appropriate covering for the VGs; it was found

that the use of 50 mil neoprene as a covering both to limit cooling losses and protect the SMA wire assemblies was sufficient to reduce power required for actuation to essentially the same level as in static (no flow) operation.

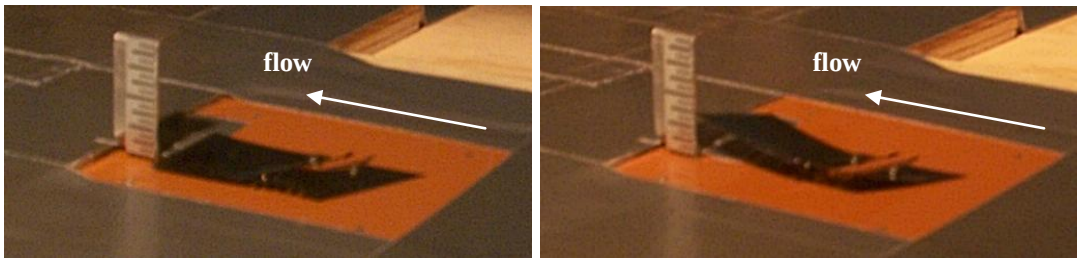

Figure 10. Low speed wind tunnel test of deployment of an individual PUVG (120 fps flow speed; 0.25" deployed height on a 1x2" PUVG).

Following additional design refinement, arrays of four PUVGs were assembled on a 12" x 3" plate for use both in tests in the low speed wind tunnel as well as for eventual installation on the wing to be used in near full scale wind tunnel testing. Figure 11 shows an early version of one such 4-PUVG array, one of several similar to those to be installed on the final wind tunnel model. Work at this stage included test installation of both powered and unpowered sets of PUVGs. The unpowered sets were used to assess the robustness of the attachment procedures, given the need to locate the attachment screws carefully to achieve the appropriate pre-buckled retracted and deployed shapes. The powered tests provided data on the repeatability of deployment and initial estimates of current levels required for deployment. Under still air conditions, roughly 3 amps of current were required for actuation, assuming .010" dia. SMA actuator wire.

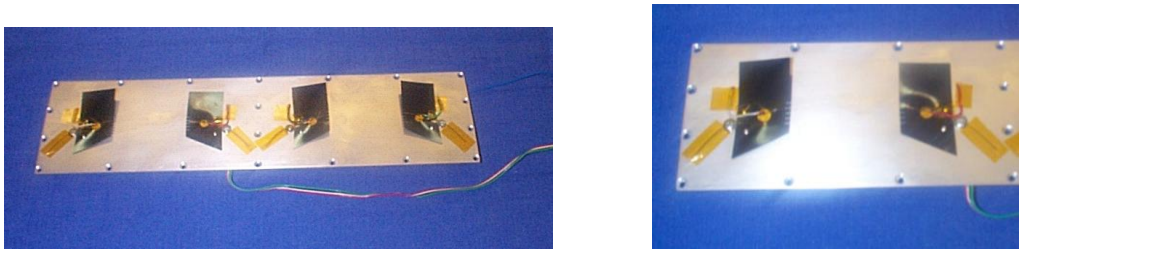

a) overall mounting of the array b) deployed (left) and retracted (right) geometries

Figure 11. Overview and details of 4-PUVG test assembly.

VI. Wind Tunnel Testing

As noted above, a 2 ft wing chord was selected as a target for near full scale testing; in addition, a NACA 23015 section was selected for this test article as being representative of airfoils used in general aviation applications. Given that a 8'x11' test section (at the G.L. Martin Wind Tunnel at the University of Maryland) was the intended test site, the final model design featured a 92" (7.67') span wing with a constant chord of 24". Figure 12 shows the wing model prior to installation as well as the aluminum endplates to be used for wall and balance interface in the tunnel as well as the location of the plates that were designed to hold the PUVG assemblies depicted in Figure 11. The wing was constructed to provide interior access for wiring to provide both power and on/off deployment control for powered VGs. Figure 13 shows the model installed in the tunnel in an as-tested configuration.

The initial tests involving measurement of model forces focused on the baseline "Basic Wing" (no PUVGs) over a range of angles of attack from -5 to 20 deg. Pre-test predictions as well as assessment of available data[35-37] on NACA 23015 airfoil performance (Figure 14) indicated that this angle of attack range would cover the relevant performance region for this foil. Note the data sources agree closely on

maximum lift for this case ($c_{\ell max}$ = ~1.2 in both cases) as well as on the increment in angle of attack between zero lift and maximum lift ($/\alpha_{\ell max} - /\alpha_{0\ell}$); this is 14.0 deg. in one case and 14.4 deg. in the other. It is of note that the post-stall behavior predicted in each case is significantly different, however.

Figure 12. Fabricated wing model, in the Basic Wing configuration, prior to installation of PUVGs.

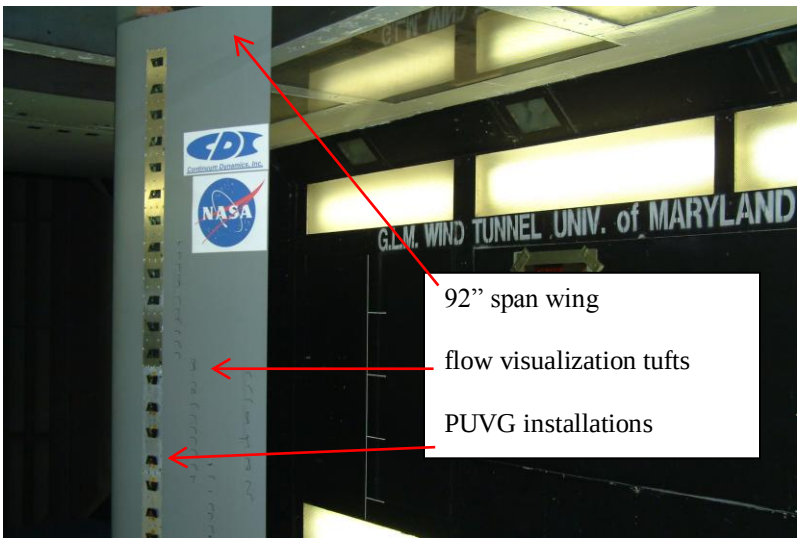

Figure 13. Overall view of vertically mounted wing model, with PUVGs installed.

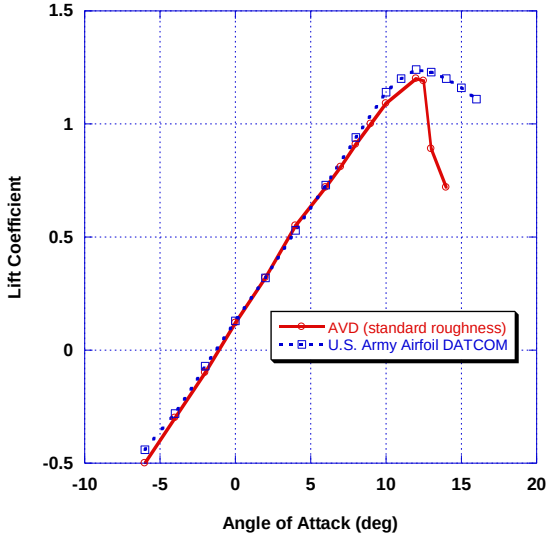

Figure 14. Lift for the NACA 23015 section (data from References 36 and 37).

Initial tests of the Basic Wing were conducted at a tunnel speed of 80 fps, corresponding to a chord Reynolds number of $1x10^6$. Measured lift coefficient, drag coefficient, and pitching moment coefficient data for the Basic Wing are summarized in Figure 15 for this case; in each plot, results of two runs are presented, showing the good repeatability typical of this test. In addition, it should be noted that owing to mechanical constraints the experimental installation involved a shift in the true angle of attack (relative to that measured by the tunnel instruments) of 1.75 deg. This accounts for the shift in the angle of attack for zero lift evident in the measured results. However, the increment from that point to maximum lift is 14.7 deg., quite close to value from the results from the literature shown in Figure 14. In addition, the peak measured lift coefficient is 1.21, quite close to the experimental result from prior tests. Both the drag and pitching moment results reflect expected trends, with a rapid rise in drag after the stall point at 15 deg. angle of attack. Also evident is a dramatic change in pitching moment coefficient (relative the 25% chord location) following stall. Flow separation over the aft portion of the foil leads to a loss of suction over the upper surface and a strong nose-down moment.

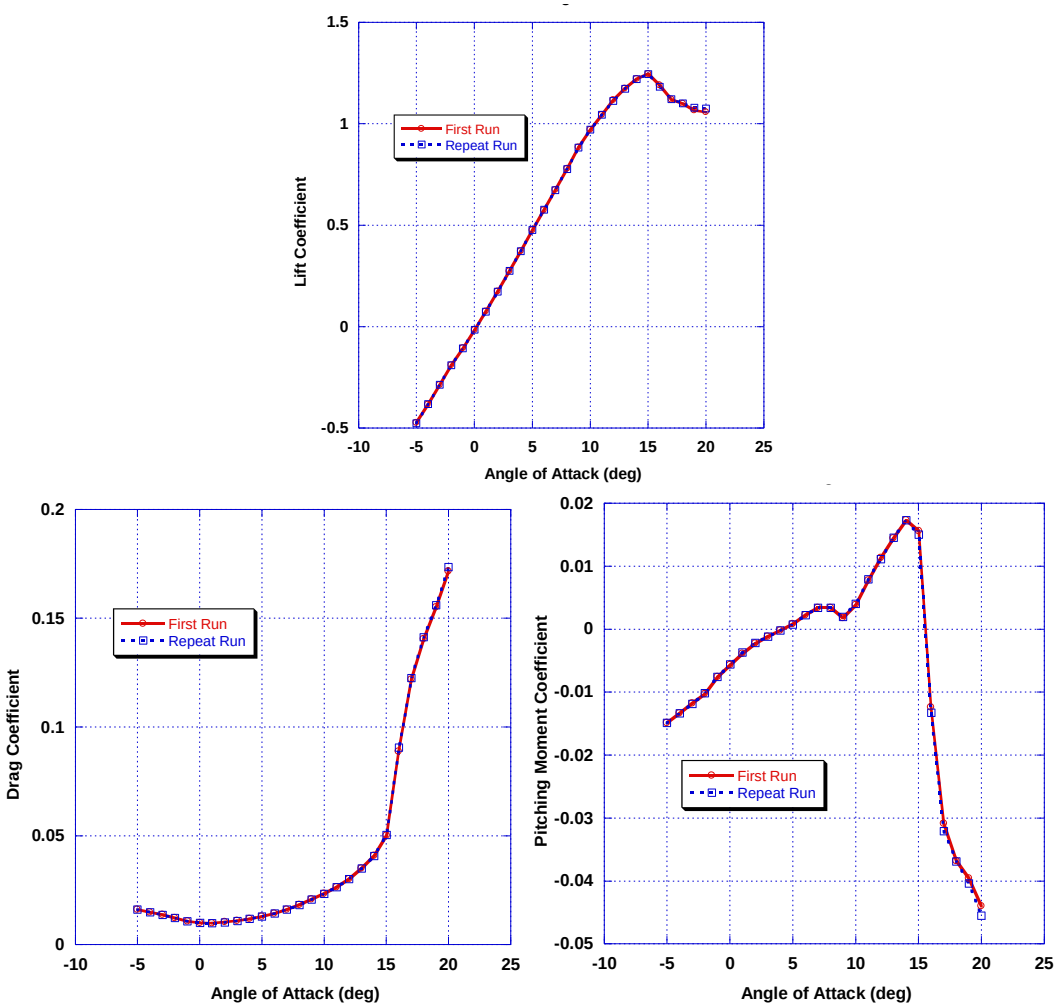

Figure 15. Lift coefficient (above), drag coefficient (above right), and pitching moment coefficient (right) vs. angle of attack: 80 fps for the "clean" Basic Wing configuration.

The next steps in testing entailed installation of PUVGs on the wing with the devices retracted and an assessment of the behavior of this case relative to the Basic Wing. As seen in Figure 16, the Basic Wing and Retracted configurations produce very similar results in terms of lift coefficient, while the Retracted case exhibits the same good repeatability as the Basic Wing. Some modest differences do arise, though, when a closeup of the peak lift coefficient region is studied.

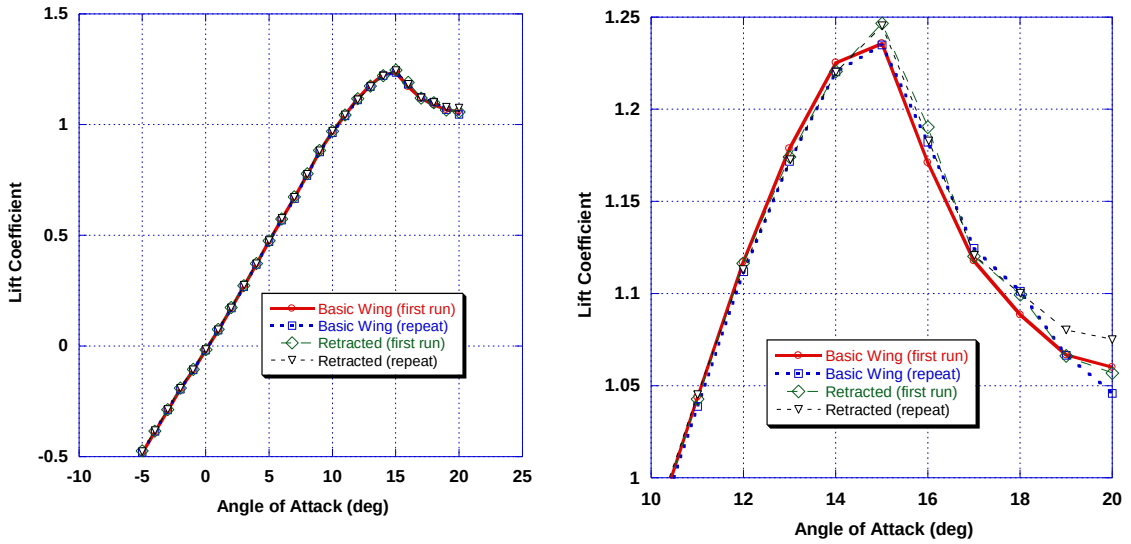

Figure 16. (Left) lift coefficient for Basic Wing and Retracted configurations; (right) closeup of measured lift coefficients for Basic Wing and Retracted configurations in the vicinity of stall.

Also of interest are comparisons of the drag generated by these two configurations. Figure 17 shows an overall drag coefficient comparison, indicating very similar results for the two cases, while the closeup in Figure 18 indicates that the Retracted case produces a small drag increase from a minimum c_d of .0099 to .00105. This 6% increase is roughly constant for the full range of angles of attack examined and is reflective of the relatively "draggy" nature of the PUVG installation when in the Retracted configuration. The as-tested mechanism, though, is susceptible of considerable improvement in this regard by a combination of fewer wire excresences and addition of a conformal covering (e.g., tape or thin neoprene). Improvements in this area are expected for the final configurations discussed below. Since the present configuration constitutes essentially a "worst case" for the PUVG, the potential payoff of the concept can be assessed in a preliminary manner given results on the effect of full PUVG deployment (see discussion at the end of this section).

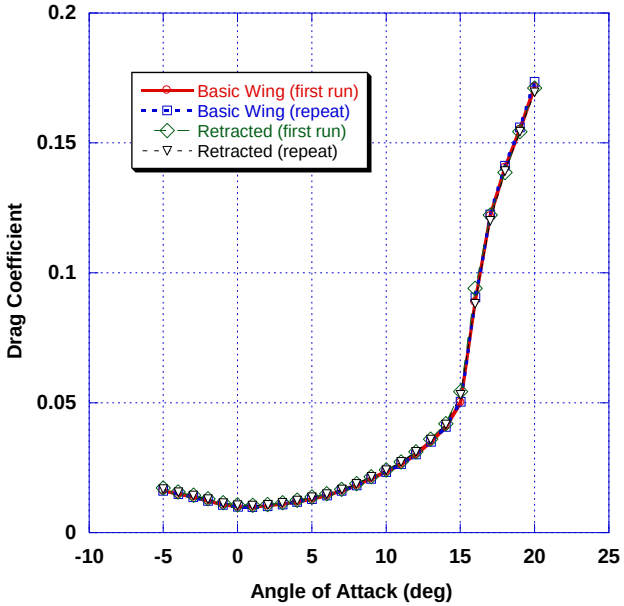

Figure 17. Drag coefficient measured for Basic Wing and Retracted configurations.

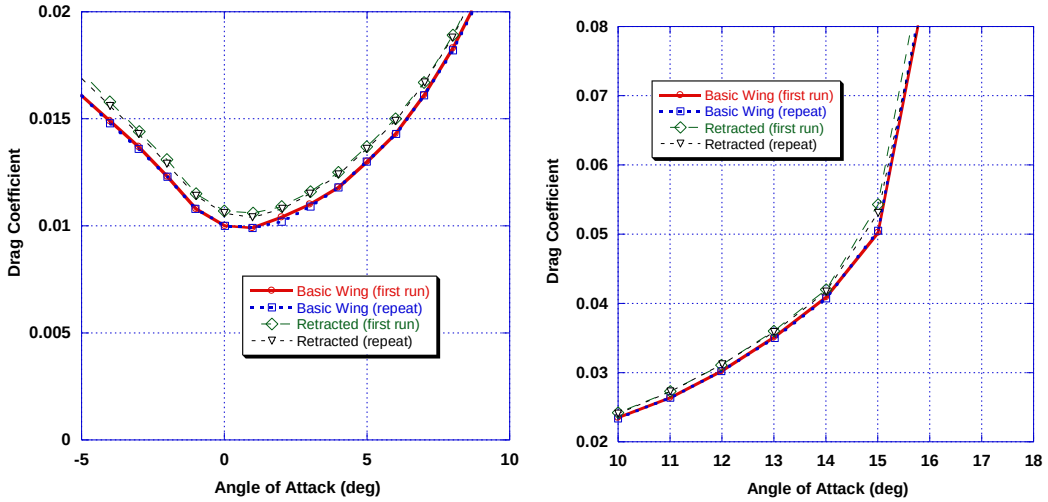

a) closeup of results at low to moderate /√v b) closeup of results at high /√v

Figure 18. Drag coefficient measured for the Basic Wing and Retracted configurations: close-ups.

The angle of attack sweep was then repeated with the PUVG array fully deployed. Figure 19 shows a photo of retracted and deployed VG positions. Once in the Deployed configuration, the lift curves shown in Figure 20 were recovered. As is evident, a very significant increment in lift is achieved, roughly 11% in maximum lift coefficient at the stall angle of attack. With respect to drag coefficient, Figure 21 summarizes this aspect of wing performance. Figure 21b shows 33% increase in minimum drag coefficient, though the increase at moderate angles of attack is roughly 25%. An interesting result, though, is that the drag coefficients of the Basic Wing a Deployed configurations at stall are very nearly equal (Figure 21a) indicating essentially no drag penalty for operating the VGs at high lift. Indeed, an important consequence of PUVG deployment is increasing lift/drag ratio at stall from 24 in the Basic Wing case to 28 in the Deployed case.

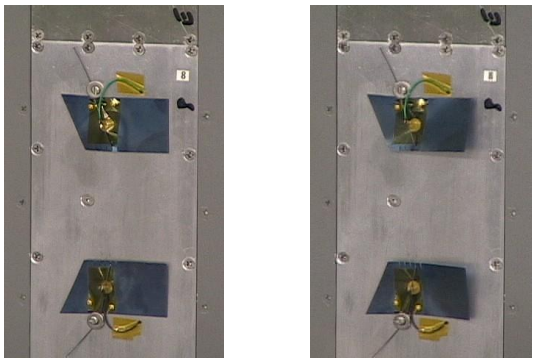

Figure 19. Closeup of retracted (left) and deployed (right) PUVG positions for one pair of the eight powered PUVGs on the test wing.

Flow visualization results that shed light on the observed behavior of integrated forces are given in Figure 22. Here, a Partially Deployed configuration is shown at various angles of attack, with the eight active VGs deployed and all other (mechanical) PUVGs left in the retracted condition. Inspection of the tuft patterns shown in Figure 22 for the angles of attack around stall clearly show the ability of the PUVGs when deployed to promote attachment; the flow downstream of the retracted VGs shows a tendency to separate earlier than does the flow downstream of the deployed PUVGs.

The key features of the wind tunnel test can be summarized by noting that the results indicate full functionality for the PUVGs over a realistic range of onset flows and angles of attack. In addition, current

and power levels that produced reliable actuation were found to be quite modest (~30 watts per device). Moreover, PUVG deployment was shown to have a marked favorable effect on wing aerodynamics, increasing maximum lift coefficient by 11% and leading to a 16% increase in lift/drag at stall. The improvement in wing performance was evident both in integrated forces on the wing as well as in visualization of flow downstream of retracted and deployed PUVG arrays. A further important aspect of these test results is that they conclusively make the case for the desirability of *deployable* PUVGs. Since deployed VGs impose a 25-33% drag penalty, while the wing profile drag penalty for retracted VGs is only 5-6%, the payoff for having a retractable device is quite strong. The ability to augment maximum lift by over 10% with a very modest cruise drag penalty and negligible weight and power penalties suggests that refinements of this design could substantially improve wing performance.

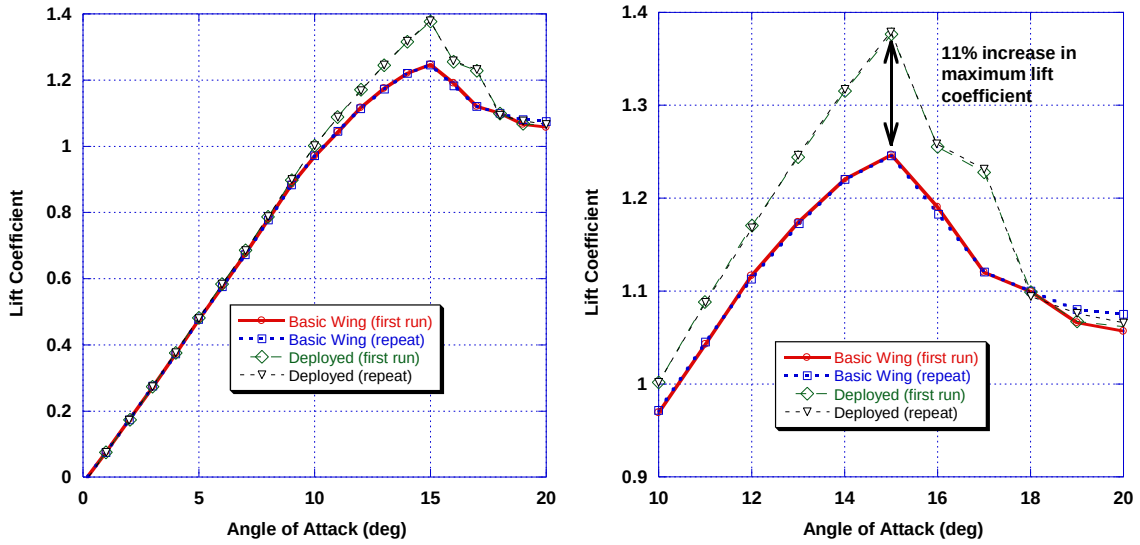

a) all angles of attack b) behavior near stall

Figure 20. Effect of PUVG deployment on maximum lift coefficient.

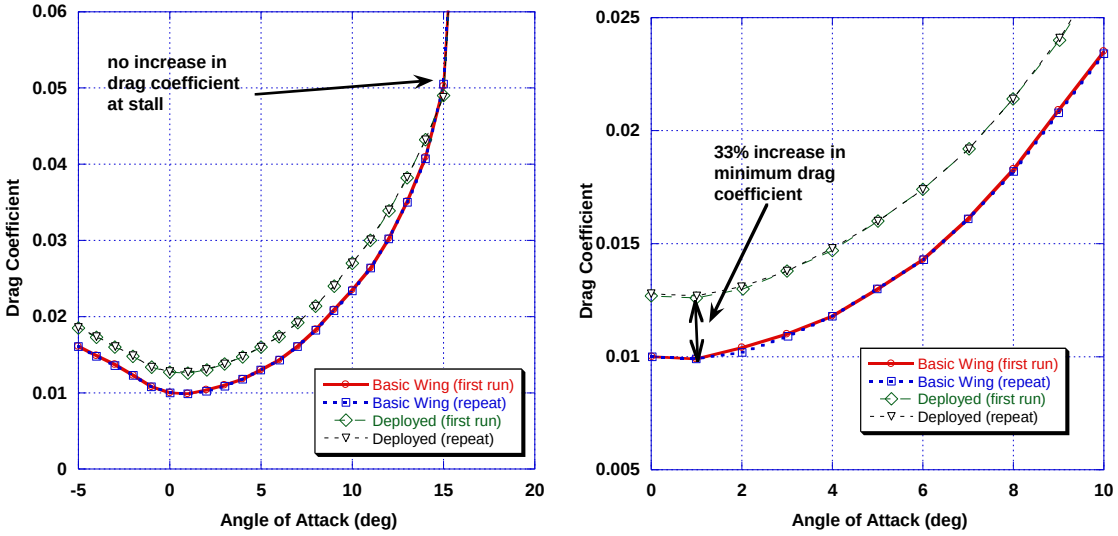

a) full results b) closeup of principal operating region

Figure 21. Drag coefficient vs. angle of attack for Basic Wing and Deployed configurations.

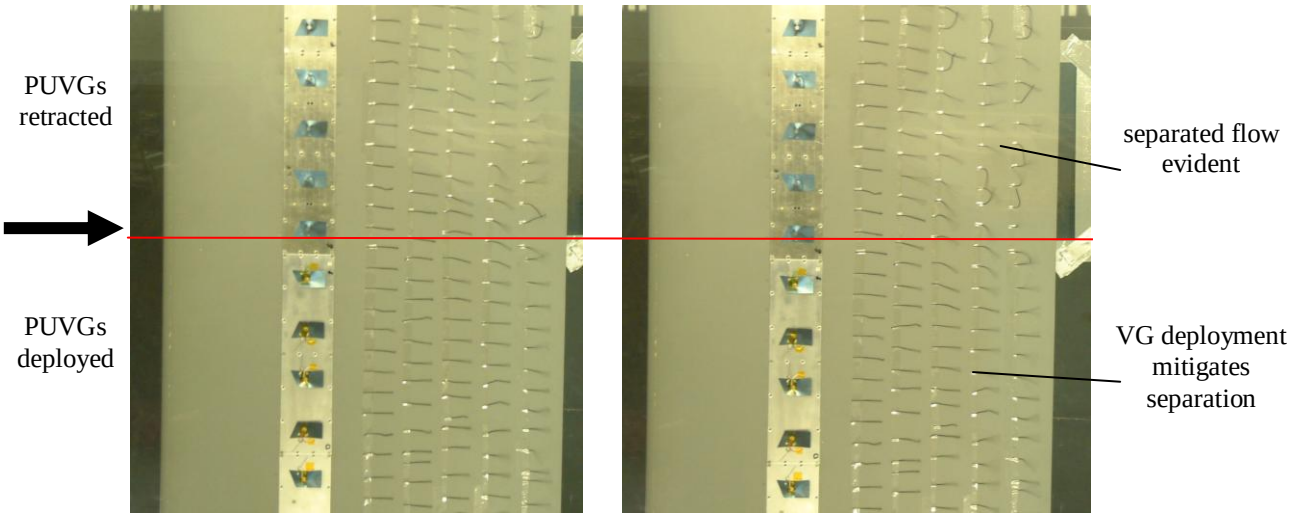

a) /ν= 15 deg. b) /ν= 16 deg.

Figure 21. Separated flow behavior and angles of attack near stall with a Partially Deployed configuration; split picture shows the effect of PUVG deployment (retracted above, deployed below).

VII. Summary

This paper has narrated the conceptual and detail design of a new class of Pop Up Vortex Generators (PUVGs) based on a novel self-locking, two-position device. General background on Shape Memory Alloy (SMA) actuation devices has been presented and the application of specially modified SMA wire actuators to the PUVGs has been described. Successful initial tests in benchtop and low speed wind tunnel environments established the functionality of the PUVGs in representative flow conditions and established current and power requirements.

These initial demonstrations set the stage for integration of multiple PUVGs on a wing operating in near full scale conditions, representative of those encountered by general aviation aircraft at landing speeds. Highlights of wind tunnel tests were presented that both defined the drag penalties associated with retracted PUVGs and demonstrated the ability of these devices to achieve up to 11% increases in maximum lift coefficient when deployed. Complementary flow visualization studies using tufts illustrated the ability of these devices to maintain attached flow when unmodified wing sections exhibited clear and dramatic separation. Given that the net drag increase at high C_L is negligible, the PUVG array system shown here offers the potential for substantially improved lift/drag ratio for wings near stall with minimal weight and power penalty. While successful in this technical demonstration, the current PUVG design can be considerably refined for real-world applications. Important priorities for follow-on design and testing include: further reduction in device height and/or adoption of recessed mounting to minimize the profile drag of the retracted configuration; additional of a suitable flexible covering the protect actuation hardware; and long-time cycle testing to establish the robustness of the mechanical design.

Acknowledgments

This work was supported by a NASA SBIR Phase II contract from NASA/Langley Research Center, contract no. NAS1-02060. The technical monitor was Mr. Julio Chu. The authors also wish to acknowledge the support of Mr. Richard Snedeker in fabrication of the wind tunnel wing model.

References

1. *Air Travel: Acquisition and Operating Cost Reduction*, web page, http://www.aero-space.nasa.gov/goals/aocr.htm, NASA Headquarters Code R, July 3, 2000.

2. Thomas, A.S.W., "Aircraft Drag Reduction Technology - A Summary," Report AGARD-R-723, AGARD, July 1985.
3. Gad-el-Hak, M. and Bushnell, D., "Status and Outlook of Flow Separation Control," AIAA-91-0037, 29th Aerospace Sciences Meeting, Reno, NV, January 1991.
4. Choi, H., Cheong, W.P, and Kim, J. "Control of Separation on Bluff Bodies," Annual Review of Fluid Mechanics, Vol. 40, pp. 113-139, January 2008.
5. Lin J. C., "Review of Research on Low-Profile Vortex Generators to Control Boundary Layer Separation," Progress in Aerospace Science, Vol.38, No. 4-5, pp. 399 – 401.
6. Bushnell, D.M., "Turbulent Drag Reduction for External Flows," Aircraft Drag Prediction and Reduction AGARD-R-723, July 1985.
7. Hefner, J.N. and Sabo, F.E., "Research in Natural Laminar Flow and Laminar Flow Control," Report NASA-CP-2487, 1987.
8. Bechert, D. W., Meyer, R., and Hage, W., "Drag Reduction of Airfoils with Miniflaps. Can We Learn from Dragonflies?," AIAA Paper 2000-2315, June 2000..
9. Saric, W.S., "Laminar Flow Control with Suction: Theory and Experiment," Aircraft Drag Prediction and Reduction AGARD-R-723, July 1985.
10. Rehman, A. and Kontis, K. "Synthetic Jet Effectiveness on Stationary and Pitching Airfoils", *Journal of Aircraft*, Vol. 43, No. 6, Nov.-Dec. 2006.
11. Gad-el-Hak, M. and Bushnell, D., "Selective Suction for Controlling Bursting Events in a Boundary Layer," AIAA Journal, Vol. 27, No. 3, pp. 308-314, March 1989.
12. Barrett, R. and Farokhi, S. "Subsonic Aerodynamics and Performance of a Smart Vortex Generator System", *Journal of Aircraft*, Vol. 33, No. 2, March-April 1996.
13. Seifert, A., Darabi, A., and Wygnanski, I., "Delay of Airfoil Stall by Periodic Excitation," Journal of Aircraft, Vol. 33, No. 4, pp. 691-698, July-August 1996.
14. Seifert, A. and Pack, L.G., "Oscillatory Control of Separation at High Reynolds Numbers," AIAA Journal, Vol. 37, No. 9, pp. 1062-1071, September 1999.
15. McManus, K.R., Legner, H.H., and Davis, S.J., "Pulsed Vortex Generator Jets for Active Control of Flow Separation," AIAA 94-2218, 25th AIAA Fluid Dynamics Conference, Colorado Springs, CO, June 20-23, 1994.
16. Wygnanski, I., "Boundary Layer and Flow Control by Periodic Addition of Momentum," AIAA-97-2117, AIAA 4th Shear Flow Control Conference, Snowmass Village, CO, June 29-July 2, 1997.
17. Wiltse, J.M. and Glezer, A., "Manipulation of Free Shear Flows Using Piezoelectric Actuators," Journal of Fluid Mechanics, Vol. 249, pp. 261-285, 1993.
18. Taylor, H.D., "The Elimination of Diffuser Separation by Vortex Generators," Report, United Aircraft Corporation, June 1947.
19. Lin, J.C., "Control of Turbulent Boundary-Layer Separation Using Micro-Vortex Generators," AIAA-99-3404, AIAA 29th Aerospace Sciences Meeting, Reno, NV, June 28 - July 1, 1999.
20. Bragg, M.B. and Gregorek, G.M., "Experimental Study of Airfoil Performance with Vortex Generators," Journal of Aircraft, Vol. 24, No. 5, pp. 305-309, 1987.
21. Wheeler, G.O.,"Means for Maintaining Attached Flow of a Flowing Medium", U.S. Patent 4,455,045, 1984.
22. Barrett,R. and Farokhi, S."On the Aerodynamics and Performance of Active Vortex Generators", AIAA Paper 93-3447-CP, 1993..
23. McKillip, R.M., Jr. and Quackenbush, T.R., "Design and Control Strategies Using Smart Structures Technology for Rotorcraft Performance Enhancement," AIAA-94-4283, September 1994.
24. *Shape Memory Wires Switch Rotary Actuator*, in *NASA Tech Notes*, July 1992.
25. Rogers, C.A., Liang, C., and Jia, J., "Structural Modification of Simply-Supported Laminated Plates Using Embedded Shape Memory Alloy Fibers," Computers and Structures, Vol. 38, No. 5/6, 1991.
26. Baz, A., Imam, K., and McCoy, J., "Active Vibration Control of Flexible Beams Using Shape Memory Actuators," Journal of Sound and Vibration, Vol. 140, No. 3, 1990.
27. McKillip, Jr., R., "Digital Tracking Tabs for One-Per-Rev Vibration Reduction," Proc. 58th AHS Annual Forum, Phoenix, AZ, June 2003.
28. McKillip, R.M., Jr. "Remotely Controllable Actuating Device", U.S. Patent No. 5,752,672, May 19, 1998.
29. Quackenbush, T.R., Bilanin, A.J., Batcho, P.F. "Implementation of Vortex Wake Control using SMA-Actuated Devices," in SPIE Smart Structures and Materials 1997, San Diego, CA, SPIE, 1997.

30. Quackenbush, T.R. and al., e. "Design, Fabrication, and Test Planning for an SMA-Actuated Vortex Wake Control System," in Proc. of the SPIE Industrial and Commercial Applications of Smart Structures Technologies Meeting, SPIE, 1998.
31. Quackenbush, T.R. and Wachspress, D.A., "Blade-Mounted Devices for Tiltrotor Performance Enhancements and Noise Reduction 99-07, CDI, Princeton, NJ, July 1999.
32. Wachspress, D.A. and Quackenbush, T.R., "Blade Vortex Interaction Noise Mitigation Via Smart Materials Technology 98-07, CDI, Princeton, NJ, July 1998.
33. Spangler, R.L., Jr. and Hall, S.R., "Piezoelectric Actuators for Helicopter Rotor Control,", 31st AIAA SDM Conference, May 1990.
34. McKillip, R.M., Jr. "Actuating Device with Multiple Stable Positions", U.S. Patent No. 6,220,550, April 24, 2001.
35. Hoerner, S.F. and Borst, H.V., 1975: Fluid Dynamic Lift, published by L.A. Hoerner.
36. Abbott, I.H., and von Doenhoff, A.E. Theory of Wing Sections, 2nd Ed., Dover Publications, 1959.
37. U.S. Army Helicopter Design DATCOM, Vol. 1 – Airfoils, USAAMRDL CR 76-2, Sept. 1976.